Analysis of the modal evolution in fused-type mode-selective fiber couplers

Gabriel Pelegrina-Bonilla,[1,2,*] **Katharina Hausmann,**[1,3] **Hakan Sayinc,**[1,3] **Uwe Morgner,**[1,2,3] **Jörg Neumann,**[1,3] **and Dietmar Kracht**[1,3]

[1] *Laser Zentrum Hannover e.V., Hollerithallee 8, D-30419 Hannover, Germany*
[2] *Institut für Quantenoptik, Leibniz Universität Hannover, Welfengarten 1, D-30167 Hannover, Germany*
[3] *Centre for Quantum Engineering and Space-Time Research (QUEST), Welfengarten 1, D-30167 Hannover, Germany*
[*] *g.pelegrina@lzh.de*

Abstract: Fused-type mode-selective fiber couplers exciting the LP_{11} mode are fabricated by well-defined fiber cladding reduction, pretapering and fusion. At a wavelength of 905 nm 80 % of the injected power in the single-mode fiber was transmitted in the few-mode fiber selectively exciting the LP_{11} mode. The coupling behavior was experimentally investigated for the case of strong as well as weak fusion. Numerical simulations based on the super-mode coupling approach were used to estimate fabrication parameters and to discuss the modal evolution in arbitrarily fused couplers. The influence of changes in the coupler geometry on the super-modes and their modal weighting are analyzed by calculations of the effective refractive index and by modal decomposition.

OCIS codes: (060.1810) Buffers, couplers, routers, switches, and multiplexers; (060.2340) Fiber optics components.

References and links

1. R.-J. Essiambre, G. Kramer, P. J. Winzer, G. J. Foschini, and B. Goebel, "Capacity limits of optical fiber networks," J. Lightwave Technol. **28**, 662–701 (2010).
2. P. J. Winzer, "Making spatial multiplexing a reality," Nature Photon. **8**, 345–348 (2014).
3. D. J. Richardson, J. M. Fini, and L. E. Nelson, "Space-division multiplexing in optical fibres," Nature Photon. **7**, 354–362 (2013).
4. J. D. Love, and N. Riesen, "Single-, few-, and multimode Y-junctions," J. Lightwave Technol. **30**, 304–309 (2012).
5. N. Riesen, and J. D. Love, "Tapered velocity mode-selective couplers," J. Lightwave Technol. **31**, 2163–2169 (2013).
6. N. Hanzawa, K. Saitoh, T. Sakamoto, T. Matsui, K. Tsujikawa, M. Koshiba, and F. Yamamoto, "Two-mode PLC-based mode multi/demultiplexer for mode and wavelength division multiplexed transmission," Opt. Express **21**, 25752–25760 (2013).
7. N. Riesen, S. Gross, J. D. Love, and M. J. Withford, "Femtosecond direct-written integrated mode couplers," Opt. Express **22**, 29855–29861 (2014).
8. S. Gross, N. Riesen, J. D. Love, and M. J. Withford, "Three-dimensional ultra-broadband integrated tapered mode multiplexers," Laser Photon. Rev. **8**, L81-L85 (2014).
9. A. A. Amin, A. Li, S. Chen, X. Chen, G. Gao, and W. Shieh, "Dual-LP_{11} mode 4×4 MIMO-OFDM transmission over a two-mode fiber," Opt. Express **19**, 16672–16679 (2011).
10. S. G. Leon-Saval, T. A. Birks, J. Bland-Hawthorn, and M. Englund, "Multimode fiber devices with single-mode performance," Opt. Lett. **30**, 2545–2547 (2005).
11. S. G. Leon-Saval, A. Argyros, and J. Bland-Hawthorn, "Photonic lanterns: a study of light propagation in multimode to single-mode converters," Opt. Express **18**, 8430–8439 (2010).

#237721 Received 8 Apr 2015; revised 28 Jul 2015; accepted 4 Aug 2015; published 24 Aug 2015

12. D. Noordegraaf, P. M. Skovgaard, M. D. Nielsen, and J. Bland-Hawthorn, "Efficient multi-mode to single-mode coupling in a photonic lantern," Opt. Express **17**, 1988–1994 (2009).
13. K. Lai, S. G. Leon-Saval, A. Witkowska, W. J. Wadsworth, and T. A. Birks, "Wavelength-independent all-fiber mode converters," Opt. Lett. **32**, 328–330 (2007).
14. A. Witkowska, S. G. Leon-Saval, A. Pham, and T. A. Birks, "All-fiber LP_{11} mode convertors," Opt. Lett. **33**, 306–308 (2008).
15. S. Matsuo, Y. Sasaki, T. Akamatsu, I. Ishida, K. Takenaga, K. Okuyama, K. Saitoh, and M. Kosihba, "12-core fiber with one ring structure for extremely large capacity transmission," Opt. Express **20**, 28398–28408 (2012).
16. B. Zhu, J. M. Fini, M. F. Yan, X. Liu, S. Chandrasekhar, T. F. Taunay, M. Fishteyn, E. M. Monberg, and F. V. Dimarcello, "High-capacity space-division-multiplexed DWDM transmissions using multicore fiber," J. Lightwave Technol. **30**, 486–492 (2012).
17. Y. Jung, R. Chen, R. Ismaeel, G. Brambilla, S. U. Alam, I. P. Giles, and D. J. Richardson, "Dual mode fused optical fiber couplers suitable for mode division multiplexed transmission," Opt. Express **21**, 24326–24331 (2013).
18. Y. Shou, J. Bures, S. Lacroix, and X. Daxhelet, "Mode separation in fused fiber coupler made of two-mode fibers," Opt. Fiber Technol. **5**, 92–104 (1999).
19. R. Ismaeel, T. Lee, B. Oduro, Y. Jung, and G. Brambilla, "All-fiber fused directional coupler for highly efficient spatial mode conversion," Opt. Express **22**, 11610–11619 (2014).
20. W. V. Sorin, B. Y. Kim, and H. J. Shaw, "Highly selective evanescent modal filter for two-mode optical fibers," Opt. Lett. **11**, 581–583 (1986).
21. K. Y. Song, I. K. Hwang, S. H. Yun, and B. Y. Kim, "High performance fused-type mode-selective coupler using elliptical core two-mode fiber at 1550 nm," IEEE Photon. Technol. Lett. **14**, 501–503 (2002).
22. K. Y. Song and B. Y. Kim, "Broad-band LP_{02} mode excitation using a fused-type mode-selective coupler," IEEE Photon. Technol. Lett. **15**, 1734–1736 (2003).
23. D. B. Mortimore, "Wavelength-flattened fused couplers," Electron. Lett. **21**, 742–743 (1985).
24. G. Pelegrina-Bonilla, K. Hausmann, K. Liu, H. Sayinc, U. Morgner, J. Neumann, and D. Kracht, "Matching of the propagation constants in an asymmetric single-mode fused fiber coupler for core pumping thulium-doped fiber at 795 nm," Opt. Lett. **37**, 1844–1846 (2012).
25. G. Pelegrina-Bonilla, K. Hausmann, H. Tünnermann, P. Weßels, H. Sayinc, U. Morgner, J. Neumann, and D. Kracht, "Analysis of the coupling mechanism in asymmetric fused fiber couplers," J. Lightwave Technol. **32**, 2382–2391 (2014).
26. S. Lacroix, F. Gonthier, and J. Bures, "Modeling of symmetric 2×2 fused-fiber couplers," Appl. Opt. **33**, 8361–8369 (1994).
27. B. S. Kawasaki, K. O. Hill, and R. G. Lamont, "Biconical-taper single-mode fiber coupler," Opt. Lett. **6**, 327–328 (1981).
28. W. K. Burns, M. Abebe, and C. A. Villarruel, "Parabolic model for shape of fiber taper," Appl. Opt. **24**, 2753–2755 (1985).
29. S. Yerolatsitis, I. Gris-Sánches, and T. A. Birks, "Adiabatically-tapered fiber mode multiplexers," Opt. Express **22**, 608–617 (2014).
30. N. Zhong, Q. Liao, X. Zhu, Y. Wang, and R. Chen, "High-quality fiber fabrication in buffered hydrofluoric acid solution with ultrasonic agitation," Appl. Opt. **52**, 1432–1440 (2013).
31. D. Marcuse, "Microdeformation losses of single-mode fibers," Appl. Opt. **23**, 1082–1091 (1984).
32. M. McLandrich, "Core dopant profiles in weakly fused single-mode fibres," Electron. Lett. **24**, 8–10 (1988).
33. C. W. Pickett, W. K. Burns, and C. A. Villarruel, "Dopant diffusion loss mechanism in high-birefringent-fiber fused couplers," Opt. Lett. **13**, 835–837 (1988).
34. E. Pone, X. Daxhelet, and S. Lacroix, "Refractive index profile of fused-fiber couplers cross-section," Opt. Express **12**, 1036–1044 (2004).
35. E. Pone, X. Daxhelet, and S. Lacroix, "Refractive index profile of fused-tapered fiber couplers," Opt. Express **12**, 2909–2918 (2004).
36. RSoft Design Group, Inc., Ossining, NY, USA, BeamPROP 8.2, 2010.
37. S. G. Leon-Saval, N. K. Fontaine, J. R. Salazar-Gil, B. Ercan, R. Ryf, and J. Bland-Hawthorn, "Mode-selective photonic lanterns for space-division multiplexing," Opt. Express **22**, 1036–1044 (2014).

1. Introduction

Single-mode fibers (SMFs) guiding only one single spatial mode are rapidly approaching their transmission capacity limit [1]. In order to delay this capacity crunch [2] various approaches have been completely optimized including wavelength-division multiplexing (WDM) and polarization-division multiplexing (PDM). Currently, the concept of space-division multiplexing (SDM) has come into focus to increase the data-carrying capacity of optical fibers [3]. This approach uses a fiber or waveguide design capable of guiding several higher-order spatial

#237721 Received 8 Apr 2015; revised 28 Jul 2015; accepted 4 Aug 2015; published 24 Aug 2015

modes instead of using a single-mode waveguide which is intrinsically limited to one spatial mode. The use of the spatial dimension as additional degree of freedom can highly increase the number of data channels. Actual devices for the application of SDM cover both fiber-based and waveguide-based approaches in order to realize spatial mode multiplexer and demultiplexer. Such waveguide-based devices include asymmetric Y-junctions [4], tapered velocity mode-selective couplers [5] and integrated asymmetric mode-selective devices [6–8]. Recently, Gross et al. [8] reported three-dimensional tapered mode-selective couplers which were written by using a femtosecond laser directly in a photonic chip. These devices exhibit extremely efficient one-to-one mode mapping with an ultra-high bandwidth.

In order to implement SDM in future fiber optical networks successfully fiber-based components are predestinated in order to achieve a high degree of compatibility with existent telecommunication systems. Despite waveguide-based approaches have advanced in recent years a lot, fiber-based solutions have still the right to exist and are actually in active development. Fiber-based solutions for this purpose are, for example, long-period gratings [9], photonic lanterns [10–12], photonic crystal fiber devices [13, 14], multicore fibers [15, 16] or mode-selective fiber couplers (MSFCs). MSFCs can be implemented with the help of few-mode fibers (FMFs) guiding several spatial modes. Such couplers can be realized as fused-type multi-mode couplers [17, 18], weakly-fused directional couplers [19], twisted fused couplers [14] or fused-type fiber couplers [20–22].

Song et al. [21] demonstrated a weakly-fused MSFC which couples the LP_{11} mode in one fiber and the LP_{01} mode in the other using a special elliptical core two-mode fiber and an SMF. A numerical analysis was done according to the evanescent field coupling approach assuming independent waveguides. Also the LP_{02} mode could be selectively excited by adequate tuning of the coupler geometry in terms of reduced cladding diameter and pretapering [22]. Generally, pretapering, which means the tapering of one fiber before both fibers are fused and pulled together, is an established method used for the fabrication of wavelength-flattened couplers [23] or couplers capable of combining two widely separated wavelengths [24]. In the latter case dissimilar fibers are used for the coupler fabrication, whereby the fiber guiding the longer wavelength is pretapered. Modal analysis of these asymmetric fused fiber couplers (FFCs) reveals that by pretapering the modal weighting of the symmetric and antisymmetric super-modes (SMs) are equalized in the coupling region, enabling a complete power transfer [25].

In this paper, fused-type MSFCs exciting the LP_{11} mode are investigated experimentally and numerically. For these investigations MSFCs were fabricated which range between weakly fusion and strong fusion. The impact of tuning the coupler geometry in terms of cladding diameter reduction, pretapering and fusion on the modal evolution of the SMs is analyzed by calculations of the effective refractive index and by modal decomposition. Therefore, the complete coupler was treated as unified structure which allowed for the calculation of the super-modes in this structure. Therefore the observed beating phenomenon could be treated according to the super-mode coupling approach. This is more general than the previous description given in [21] for MSFCs based on the evanescent field coupling approach, since the super-mode coupling approach is, as opposed to the evanescent field coupling approach, also valid for well-fused couplers, where the modes of each fiber cannot be treated independently anymore. Although FFCs have already been analyzed in terms of super-modes [26] the presented work expands the analysis to the general case of asymmetric FFCs where two different types of fibers are used. This allows for the modeling of for example MSFCs. The super-mode coupling approach removes the limitation of independent waveguides in the evanescent field coupling approach and enables the analysis of arbitrarily fused MSFCs in general. Treating MSFCs with the super-mode coupling approach was recently highlighted to be an open topic which should be addressed in future research [19].

#237721 Received 8 Apr 2015; revised 28 Jul 2015; accepted 4 Aug 2015; published 24 Aug 2015

2. Experimental realization

2.1. Fabrication

The presented experiments were realized at a wavelength of 795 nm using different standard circular-core fibers, a 630-HP (cladding diameter = 125 µm, core diameter = 3.5 µm, NA = 0.13) and a 1310BHP (cladding diameter = 125 µm, core diameter = 8.5 µm, NA = 0.13). At a wavelength of 795 nm the 630-HP guides only the fundamental LP_{01} mode and acts therefore as SMF. At this wavelength the 1310BHP guides the LP_{01} mode and several higher-order modes (HOMs) and acts therefore as FMF. The specific wavelength of 795 nm was chosen, due to the availability of SMFs and FMFs. However, the obtained results are transferable to arbitrary wavelengths including typical telecommunication wavelengths. Figure 1 illustrates the function of an MSFC, where the LP_{01} mode launched into the SMF selectively excites an HOM in the FMF, i. e. the LP_{11} mode or the LP_{21} mode.

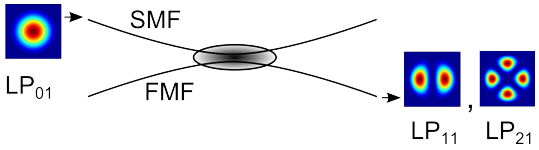

Fig. 1. Mode-selective fiber coupler (MSFC) consisting of a single-mode fiber (SMF) and a few-mode fiber (FMF). The fundamental LP_{01} mode is launched into the SMF and can selectively excite HOMs in the FMF, i. e. the LP_{11} mode or the LP_{21} mode.

A standard fused biconical taper technique [27] was used for the fabrication of the MSFCs. The region which is softened during the heating process, called hot zone [28], was determined to be $\Delta z \approx 7$ mm in our configuration. Further details concerning the fabrication process are given in [25] where the same configuration was used.

Both fibers were etched with 40 % hydrofluoric acid to a diameter of about 40 µm $\pm$ 5 µm prior to the coupler fabrication. The fabrication of the MSFCs started with the pretapering process where only the SMF was tapered for a certain extension (pretaper length). Etched cladding diameter and pretaper length were estimated based on simulations which will be discussed later on. Afterwards both fibers were twisted, heated and pulled, while the transmission at both fiber outputs was monitored with photodiodes. In addition, the near-field output intensity pattern at the FMF end was monitored simultaneously to the transmitted power with the aid of a focusing lens, a beam splitter and a CCD camera.

2.2. Characterization

In Fig. 2 the experimentally recorded transmission at the output of the SMF and FMF during the pulling process (pulling signature) is depicted. In the non-pretapered case (cf. Fig. 2(a)) no power is coupled to the FMF. When a pretaper length of 3.5 mm (taper diameter of 32 µm) was applied on the SMF (cf. Fig. 2(b)) a substantial increase of the maximum coupled power from the LP_{01} mode guided in the SMF to the LP_{11} mode in the FMF was observed. At the beginning of the pulling process at an extension of 5.4 mm an intensity pattern corresponding to the LP_{21} mode was detected whereby the transmitted power was only 1 %. With further pulling a maximum at an extension ranging from 7 to 12 mm was detected with a transmitted power of maximal 45 %. The intensity pattern shows a selective excitation of the LP_{11} mode. At an extension of 12.7 mm the transmission in the LP_{11} mode was 66 %. A further coupling cycle was detected at 13.5 mm extension showing a more annular mode rather than a two-lobed LP_{11} mode. Due to the fact that a circular-core FMF was used, mode coupling between the

#237721 Received 8 Apr 2015; revised 28 Jul 2015; accepted 4 Aug 2015; published 24 Aug 2015

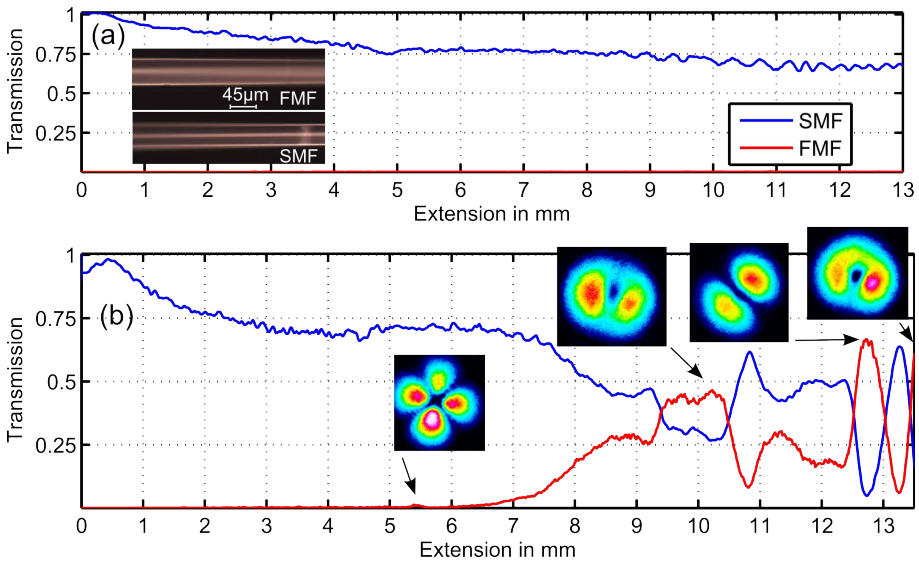

Fig. 2. Experimentally measured transmission at a wavelength of 795 nm at the output of the SMF and FMF during the fabrication process for the non-pretapered case (a) and for the case that a pretaper length of 3.5 mm is applied on the SMF (b). The inset in (a) shows optical microscope photographs taken at a magnification of x100 of the FMF and SMF after the etching process. The insets in (b) are showing the intensity pattern at the FMF end at the indicated extension.

90°-rotated versions of the LP_{11} modes can occur [29]. The ring-shaped intensity patterns in Fig. 2(b) indicate this coupling behavior.

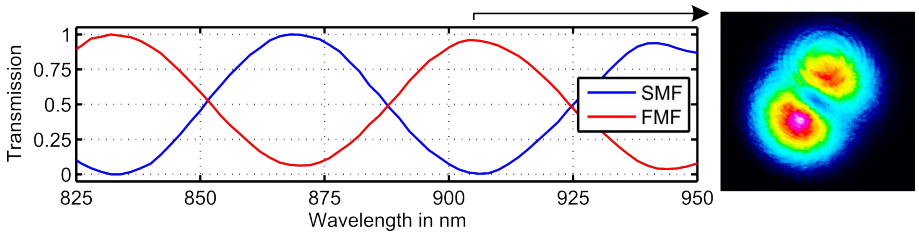

Fig. 3. Wavelength dependence of the fabricated MSFC. The data points were normalized to the overall transmitted power. At a wavelength of 905 nm 80 % of the injected power was transmitted in the FMF.

The pulling process was stopped at an extension of 13.55 mm for further packaging of the coupler. Upon completion of the pulling process the coupling ratio changed, so that 60 % of the overall transmitted power was in the FMF and 40 % in the SMF. Therefore this MSFC is not suitable for an efficient LP_{11}-excitation at a wavelength of 795 nm. The spectral characteristics of this MSFC were measured with an optical fiber analysis system (Photon Kinetics 2500) and the results are shown in Fig. 3. The transmission is maximal in the FMF at wavelengths of 832 and 905 nm. The selective LP_{11}-excitation was verified at a wavelength of 905 nm (cf. intensity pattern in Fig. 3) and it was measured that 80 % of the injected power was transmitted in the FMF.

#237721 Received 8 Apr 2015; revised 28 Jul 2015; accepted 4 Aug 2015; published 24 Aug 2015

2.3. Discussion of the loss mechanisms

Both cases, non-pretapered and pretapered, have in common that at the beginning of the tapering process part of the launched power is irrecoverably lost. It was measured that the power transmitted in the SMF decreases during the pulling process to less than 75 % although no power is coupled to the FMF. This loss during the pulling process was observed in several of our experiments. We think that the loss might be attributed to fiber damage during the etching process [30], microbends [31], core dopant diffusion [32] or a combination of these loss mechanisms.

The inset in Fig. 2(a) shows optical microscope photographs taken at a magnification of x100 of the used fibers after the etching process. No obvious fiber damage as micro-cracks or microdeformations on the surface are visible for this fiber pair which was used for the experiment presented in Fig. 2(a). The general quality of the etched fibers was verified with SEM images to be good and only fibers without visible damage were used for the experiments. Nevertheless, it cannot be excluded that fiber damage introduced by the etching process leads to losses during the coupler fabrication. In addition, microscopic bends [31] of the fibers can occur during the fusion process leading to bending losses. These microbending losses get pronounced since very thin (etched) fibers are used.

Another source of losses can be the diffusion of core dopants due to the application of a high temperature and axial tension which reduces the core-cladding index difference and increases the core diameter [18, 32]. Pickett et al. [33] identified this effect as loss mechanism which occurs in the fabrication of couplers due to nonadiabatic transitions of the core-guided mode at the input and output sections of the fiber taper. The transition must be adiabatic in order to prevent uncontrollable mode coupling to higher-order cladding modes and to be low loss. We tried to minimize the influence of this effect by running the tapering process at the lowest possible temperature.

2.4. Impact of the degree of fusion

The temperature during the fabrication process has a major impact on the degree of fusion (DoF). The DoF is defined as $\mathrm{DoF} = \frac{2 \cdot z}{x+y}$, where x is the diameter of the SMF, y the diameter of the FMF and z the width of the structure in the taper waist. In this definition a DoF of 1 means complete fusion and a DoF of 2 means no fusion. The coupler realized for Fig. 2(a) was pulled up to an extension of 13.7 mm, cleaved at the taper waist and examined under an optical microscope, measuring a DoF of 1.75. For the pulling signature in Fig. 2(b) no information about the DoF is available, since the coupler was housed for further characterization. Based on experiments with the same parameters we estimate the DoF to be in the order of 1.70 ± 0.05 and therefore well-fused.

In order to evaluate the influence of the DoF on the coupler behavior, we recorded the pulling signature of a weakly-fused MSFC with a DoF of 1.98 (cf. Fig. 4(a)). No coupling was detected in the weakly-fused case in comparison to the coupler with a DoF of approximately 1.7 (cf. Fig. 2(b)). The applied pretaper length on the SMF was 3 mm for the coupler shown in Fig. 4(a) and 3.5 mm for the coupler shown in Fig. 2(b). Therefore the applied pretaper length is not exactly equal, but this difference in terms of the pretaper length should have only a minor influence on the coupling behavior. In addition, a strongly-fused MSFC applying a pretaper length of 3.5 mm was pulled with a DoF of 1.5 whose pulling signature is depicted in Fig. 4(b). In this case the LP_{11} mode could be selectively excited at extensions of 6 and 8.5 mm with more than 40 % transmission. Compared to the pulling signature for the case with a DoF of 1.7 (cf. Fig. 2(b)) this one is different in terms of transmission and extension of each overcoupling maximum.

These results point out how sensitive the coupler fabrication is to variations of the coupler geometry. Besides a cladding diameter reduction and an appropriate pretaper length, also the right

#237721 Received 8 Apr 2015; revised 28 Jul 2015; accepted 4 Aug 2015; published 24 Aug 2015

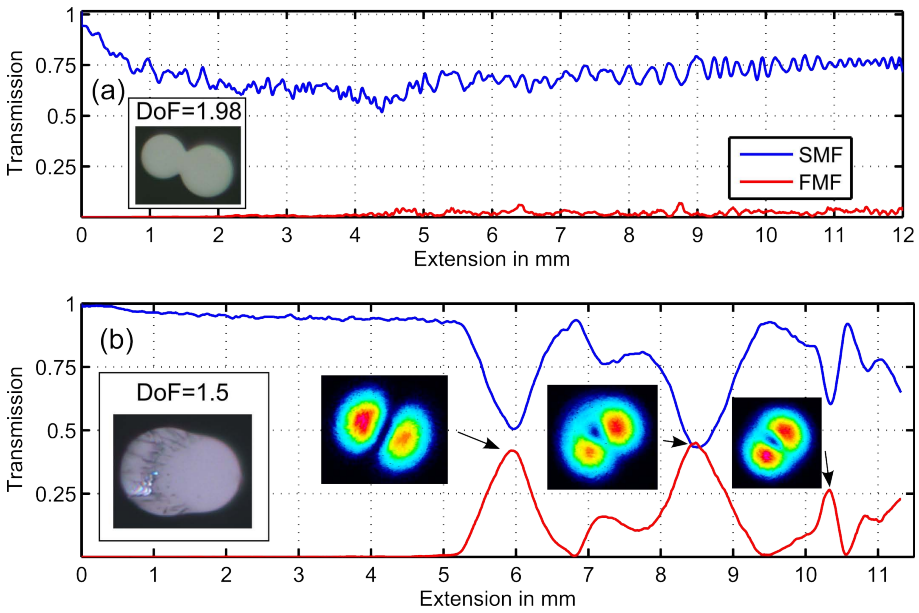

Fig. 4. Experimentally measured transmission at a wavelength of 795 nm at the output of the SMF and FMF during the fabrication process for a pretaper length of 3 mm with a DoF of 1.98 (a) and for a pretaper length of 3.5 mm and a DoF of 1.5 (b). The insets show a photograph of the cleaved taper waist. The insets in (b) show the intensity pattern at the FMF end at the indicated extension.

choice of the DoF is crucial for an efficient excitation of HOMs. Ismaeel et al. [19] discussed weakly-fused couplers based on inter-modally phase-matching the propagation constants in each arm of the asymmetric fused coupler. In the weakly-fused case both arms can be considered isolated and due to the small fused region the fields in both arms can overlap. As stated in [19] a stronger fusion will make it more difficult to find the right phase matching condition since both fibers will become a combined structure and cannot be considered isolated. Also the results shown in [20] and [21] were obtained only for weakly-fused couplers and were theoretically treated according to the evanescent field coupling approach. The couplers pulled for Fig. 2 and 4 exhibit a much stronger degree of fusion so that independent waveguides cannot be assumed. For this reason the coupler structure has to be considered as unified structure and it is necessary to use the super-mode coupling approach in order to perform a modal analysis of the resulting waveguiding structure in terms of effective refractive index considerations and modal decomposition.

3. Numerical investigations

We modeled the behavior of the fabricated MSFCs by using our own three-dimensional (3D) FFT-based beam propagation method (BPM) algorithm. This model considers the complete unified coupler structure and is not limited to the assumption of isolated waveguides. In [25] the model was successfully used to analyze the modal evolution and coupling mechanism in asymmetric FFCs for WDM applications. Due to simplifications in terms of material conservation the model has some issues when strongly-fused couplers with a DoF below 1.4 are considered. The material conservation was considered perfectly by Pone et al. [34, 35], who developed a sophisticated model for the calculation of the refractive index profile of FFCs by solving the

#237721 Received 8 Apr 2015; revised 28 Jul 2015; accepted 4 Aug 2015; published 24 Aug 2015

diffusion-convection equation. Since in this case MSFCs with a DoF above 1.5 are investigated, our model should provide useful information about the light propagation and encourage a discussion of the modal evolution in these couplers.

3.1. Simulation of the transmitted power

For the fabrication of MSFCs detailed information about the fabrication parameters as cladding diameter, pretaper length and DoF are indispensable. Therefore the complete transmission in the FMF, when light was launched into the SMF, was calculated depending on the pretaper length of the SMF and the extension. Cladding diameters of 45 µm for both fibers were assumed and the well-fused case with a DoF of 1.7 (cf. Fig. 5(a)) and the weakly-fused case with a DoF of 1.95 (cf. Fig. 5(c)) were chosen.

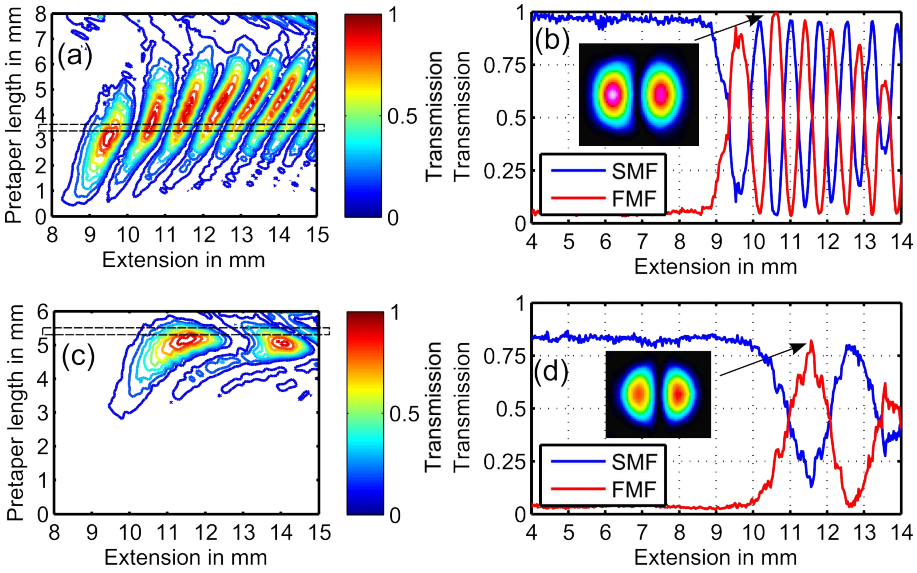

Fig. 5. Simulated transmission in the FMF, when light was launched into the SMF, for cladding diameters of 45 µm for both fibers. Well-fused case with a DoF of 1.7 (a) and weakly-fused case with a DoF of 1.95 (c). Pulling signature at a pretaper length of 3.5 mm in the well-fused case (b) and at a pretaper length of 5.37 mm in the weakly-fused case (d).

In the non-pretapered case no power is coupled to the FMF no matter if the coupler was well-fused or weakly-fused. By increasing the pretaper length to values between 2 and 5 mm the maximal coupled power from the SMF to the FMF was substantially increased in the well-fused case. In Fig. 5(b) the pulling signature at a pretaper length of 3.5 mm is depicted, demonstrating a complete power transfer and excitation of the LP_{11} mode at an extension of 10.6 mm.

In the weakly-fused case the pretaper length must be further increased to values between 4.5 and 5.5 mm in order to achieve a significant power transfer. The respective pulling signature at a pretaper length of 5.37 mm (taper diameter of 28 µm) is depicted in Fig. 5(d) and shows a transmission of approx. 80 % in the FMF at an extension of 11.6 mm exciting the LP_{11} mode. In comparison to the well-fused case the coupling behavior is different with respect to the number and the position of the coupling cycles. Therefore, the optimal pretaper length for achieving a complete power transfer and LP_{11}-excitation depends on the DoF.

The simulations confirmed qualitatively the experimentally observed impact of reduced cladding diameter, pretaper length and the DoF on the selective excitation of the LP_{11} mode.

#237721 Received 8 Apr 2015; revised 28 Jul 2015; accepted 4 Aug 2015; published 24 Aug 2015

A comparison of the experimental (cf. Fig. 2) and simulation (cf. Fig. 5) results shows a qualitative agreement between both, since the essential features, as LP_{11}-excitation and maximum coupled power, are explained by the simulation. Although, the simulation does not account for the exact position, in terms of transmitted power and extension, of each overcoupling maximum. This is due to the simplified refractive index profile in the simulation, which neglects the material conservation, and the fact that it is difficult to take all experimental parameters into account.

3.2. Calculation of super-modes

In order to understand the coupling behavior in well-fused and strongly-fused MSFCs the fibers cannot be evaluated separately and the SMs have to be calculated for the whole cladding structure according to the super-mode coupling approach. For the calculation of the eigenmodes we used the built-in mode solver utility of BeamPROP [36]. Figure 6 shows the six lowest-order SMs of the coupler structure at the beginning of the taper and the taper waist, defined by the respective propagation constant in descending order. The modes were calculated for a coupler with the same parameters used in Fig. 5(b) and at an extension of 10.6 mm.

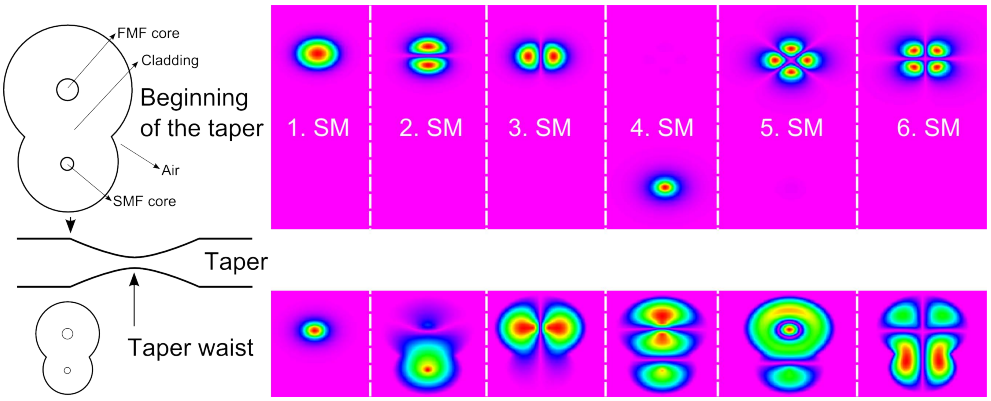

Fig. 6. Six lowest-order SMs of the coupler structure at the beginning of the taper and the taper waist, defined by the respective propagation constant in descending order. The modes were calculated for a coupler with the same parameters used in Fig. 5(b) and at an extension of 10.6 mm.

At the beginning of the taper the first SM corresponds to the LP_{01} mode of the FMF and the second and third SMs are the two 90°-rotated versions of the LP_{11} mode. The fourth SM corresponds to the LP_{01} mode of the SMF. The fifth and sixth SMs correspond to the two 45°-rotated versions of the LP_{21} mode of the FMF. The seventh SM (not shown here) corresponds to the LP_{02} mode core guided in the FMF and all further eigenmodes are cladding modes.

In symmetric fiber devices, as FFCs and photonic lanterns, light launched into one fiber core excites all SMs or in other words the guided core mode is a superposition of all SMs. The number of the excited SMs equals the number of the fiber cores [11]. In the asymmetric case, where the cores have different radii and numerical apertures, the SMs at the beginning of the taper correspond to the respective core modes of the fibers. This means that in this case light launched into the SMF will only excite the fourth SM. Since in the case of a MSFC the idea is to achieve mode coupling, for example to the LP_{11} mode (respectively to the second SM), this mode has to be excited along the propagation in the coupler.

As long as the SMs are core guided each of them can be easily assigned to an LP-mode. Along the propagation to the taper waist the SMs will consecutively evolve into cladding modes

#237721 Received 8 Apr 2015; revised 28 Jul 2015; accepted 4 Aug 2015; published 24 Aug 2015

(except for the first SM in this case) which are remarkably different from the SM at the beginning of the taper so that the corresponding LP-mode cannot be simply assigned.

3.3. *Evolution of the effective refractive index n_{eff}*

In the following the effective refractive indices n_{eff} of the six lowest-order SMs along the propagation in the taper are calculated (cf. Fig. 7(a)) for a coupler with the same parameters used in Fig. 6. This calculation can reveal at which position in the taper, mode coupling between the SMs can occur due to matched propagation constants.

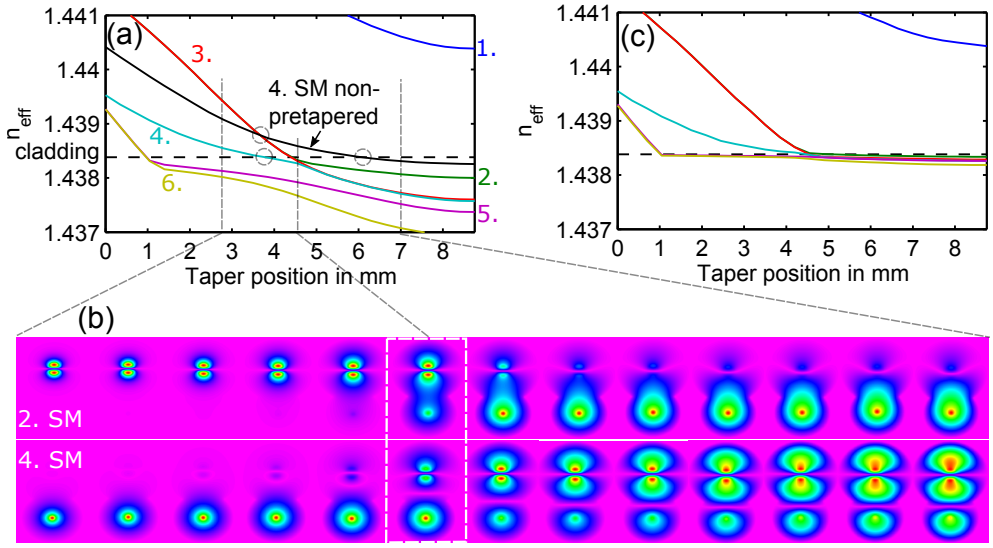

Fig. 7. (a) Evolution of the effective refractive index n_{eff} of the n-th SM along the taper position for a coupler with the same parameters used in Fig. 6 and (c) with a cladding diameter of 125 µm. (b) Second and fourth SM at a taper position between 2.8 and 7 mm. The simulated cross section is consecutively rescaled.

Since light is launched into the SMF, the fourth SM is excited at the beginning of the taper. At a taper position of 3.8 mm the n_{eff} of the fourth SM equals the cladding refractive index which means that the mode is no more guided in the core and becomes a cladding mode. With further progression the n_{eff} approximates the n_{eff} curves of the 90°-rotated versions of the LP_{11} mode at a taper position of 4.5 mm. If the n_{eff} of the SM cross or interact with each other during the taper transition, mode coupling between the respective SMs can occur [37]. Therefore, in the pretapered-case mode coupling between the fourth SM and the LP_{11} mode set, which correspond to the second and third SM, can occur. At this point the LP_{11} mode set becomes non-degenerated, because both SMs evolve into cladding modes of a non-circular refractive index structure. Figure 7(b) shows the evolution of the second and fourth SM at a taper position between 2.8 and 7 mm. At the taper position of 4.5 mm where the n_{eff} curves are closest to each other, both SMs expand into the whole cladding structure. The second and fourth SM seem to be a combination of both, the LP_{11} mode located at the FMF and the LP_{01} mode located at the SMF.

In Fig. 7(a) the n_{eff} curve for the fourth SM in the non-pretapered case is also depicted. In this case the fourth SM breaks out of the core at a higher values of the taper position of 6.1 mm and the n_{eff} curve does not approximate any other n_{eff} curve of a higher-order SM after the core-cladding transition. At a taper position of 3.7 mm the n_{eff} curve crosses the n_{eff} curves of

#237721 Received 8 Apr 2015; revised 28 Jul 2015; accepted 4 Aug 2015; published 24 Aug 2015

the LP_{11} mode set and becomes the second SM. Note, that at this intersection the LP_{01} mode in the SMF is core guided and that a power transfer to the FMF can take place only due to evanescent field coupling. For this, the cores have to be in near proximity which is apparently not the case, since no coupling occurs (cf. Fig. 5(a)).

Figure 7(a) also illustrates qualitatively why it is necessary to pretaper the SMF. Due to pretapering it can be achieved that the initially excited SM breaks out of the core and subsequently approximates the n_{eff} curves of the targeted SM; in this case the LP_{11} mode corresponding to the second SM. Further pretapering could therefore result in the excitation of modes having a higher order, but is practically limited by the mechanical handling of a strongly pretapered fiber. Alternatively, a FMF with a higher V-parameter could be used which would shift the n_{eff} curves of the HOMs to higher values of the taper position avoiding the practically inconvenient strong pretapering of the SMF. These considerations also indicate that by pretapering the FMF instead of the SMF, coupling between the fourth SM and the first SM can be achieved, which was demonstrated in [25].

These findings are valid for arbitrary wavelengths and can be transferred to telecommunication wavelengths. However, the progression of the n_{eff} curves changes according to the considered wavelength. For higher wavelengths the n_{eff} curves will shift to the left because the SMs will break out of the core at lower taper positions and also the progression itself will change due to the modified cladding diameter in the cladding guided region. The limits for increasing the wavelengths are given by the guidance of the fundamental mode in the SMF and the LP_{11} mode in the FMF. The behavior for shorter wavelengths is considered respectively.

In addition to an adequate choice of the pretaper length, it is necessary for the fabrication of MSFCs to reduce the cladding diameter of common fibers with 125 µm cladding diameter for example by etching. The evolution of the n_{eff} along the taper position for fibers with a 125 µm cladding diameter is depicted in Fig. 7(c). In comparison to the case with 45 µm cladding diameter all n_{eff} curves overlap after the core-cladding-transition which results in strong coupling between all these SMs making it impossible to selectively excite one of them. A reduction of the cladding diameter will pronounce the refractive index of the surrounding material and will therefore split up the n_{eff} curves allowing a selective excitation of the desired mode.

3.4. Modal decomposition

The considerations concerning the n_{eff} curves are valuable to qualitatively discuss the excitation of SMs and the coupling between them. Although, they cannot definitely reveal if a SM is excited or not. Therefore, we performed a modal decomposition of the simulated light field. The light propagation was simulated by our FFT-based BPM algorithm and for the calculation of the eigenmodes we used the built-in mode solver utility of BeamPROP. The simulated field E_{sim} was decomposed on the calculated eigenmodes E_i by projecting the simulated field on the eigenmodes with the coefficients c_i given by:

$$c_i = \frac{\iint E_{\mathrm{sim}}(x,y) \cdot E_i^*(x,y)dxdy}{\sqrt{(\iint |E_{\mathrm{sim}}(x,y)|^2 dxdy) \cdot (\iint |E_i(x,y)|^2 dxdy)}}. \tag{1}$$

These complex coefficients can be used to calculate the reconstructed field E_{rec} as weighted superposition of the calculated eigenmodes E_i with

$$E_{\mathrm{rec}}(x,y) = \sum_{i=0}^{N} c_i \cdot E_i(x,y) \tag{2}$$

and the modal weight of each eigenmode is then given by $|c_i|^2$.

In Fig. 8(a) the modal excitation along the coupler with the same parameters used in Fig. 6 and 7 is depicted. At the beginning of the taper up to a taper position of 4 mm only the fourth

#237721 Received 8 Apr 2015; revised 28 Jul 2015; accepted 4 Aug 2015; published 24 Aug 2015

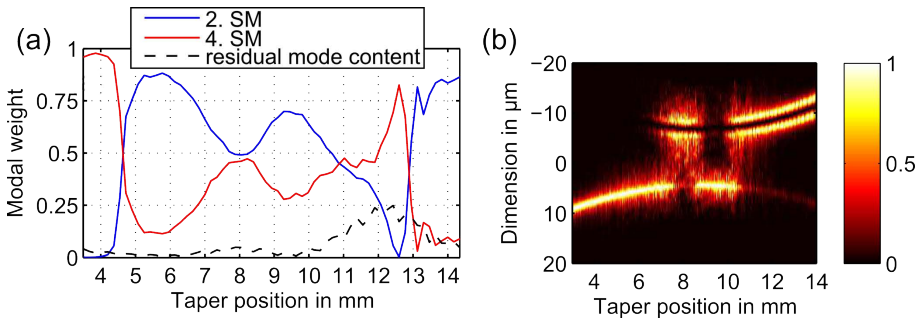

Fig. 8. Modal excitation (a) and light propagation (b) along a coupler with an extension of 10.6 mm and a pretaper length of 3.5 mm. The light was launched into the SMF (bottom). The data points of each propagation slice were scaled to their respective maximum.

SM is excited, because the light is launched into the SMF. At a taper position of 4 mm the modal weight changes up to the point at 4.6 mm where both SMs are equally excited. This zone corresponds to the part in Fig. 7(a) where the fourth SM breaks out of the core and the n_{eff} curves approximate each other. On the up-taper part at a taper position of 12.8 mm the light is recaptured by the cores and mainly the LP_{11}-corresponding second SM persists excited. The corresponding light propagation is shown in Fig. 8(b) demonstrating the mode conversion from the LP_{01} mode to the LP_{11} mode and the mode beating in the taper waist. The data points of each propagation slice were scaled to their respective maximum. The modal weighting of the involved SMs in the cladding guided regime between 4.6 and 12.8 mm changes along the taper position which is due to the evolution of the SMs shown in Fig. 7(a) and the resulting mode beating.

3.5. Impact of the degree of fusion

In comparison to the so far discussed well-fused couplers, we will analyze in the following the modal evolution in weakly-fused couplers, i. e. having a DoF of 1.95. In Fig. 9 the evolution of the n_{eff} is depicted with the same pretaper length and parameters (cf. Fig. 7) as in the well-fused case (a) and at an optimized pretaper length of 5.37 mm (b) as obtained from Fig. 5(c).

The trend of the n_{eff} curves in Fig. 9(a) is similar to the well-fused case, although the fourth SM shows the same behavior as the n_{eff} curve of the non-pretapered case in Fig. 7(a). The n_{eff} curve of the initially fourth SM becomes the second SM and intersect the n_{eff} curves of the LP_{11} mode set at a position of 4.5 mm, but no coupling occurs at this taper position (cf. Fig. 5(c)). The evolution of the second and fourth SM is depicted in Fig. 9(c) and reveals that along the taper the respective SMs remain localized in the fiber where they were initially launched. Therefore, the chosen pretaper length of 3.5 mm seems to be inappropriate for this DoF.

A change of the pretaper length to 5.37 mm leads to an outbreak of the fourth SM at a lower taper position of 2.8 mm (cf. Fig. 9(b)). The fourth SM and the LP_{11}-corresponding mode set approximate each other at a taper position of 5.6 mm. In contrast to the case with a pretaper length of 3.5 mm the LP_{11} mode set becomes non-degenerated. The evolution of the second and fourth SM, shown in Fig. 9(d), demonstrates that at this position both SMs expand into the whole cladding structure. Therefore, light launched into the SMF should excite both SMs at this point.

The modal excitation of both SMs along the coupler is depicted in Fig. 10(a) and demonstrates that at this position the modal weighting of the second and fourth SM are equal. On the up-taper part at a taper position of 12.1 mm the light is recaptured by the cores and at the end of

#237721 Received 8 Apr 2015; revised 28 Jul 2015; accepted 4 Aug 2015; published 24 Aug 2015

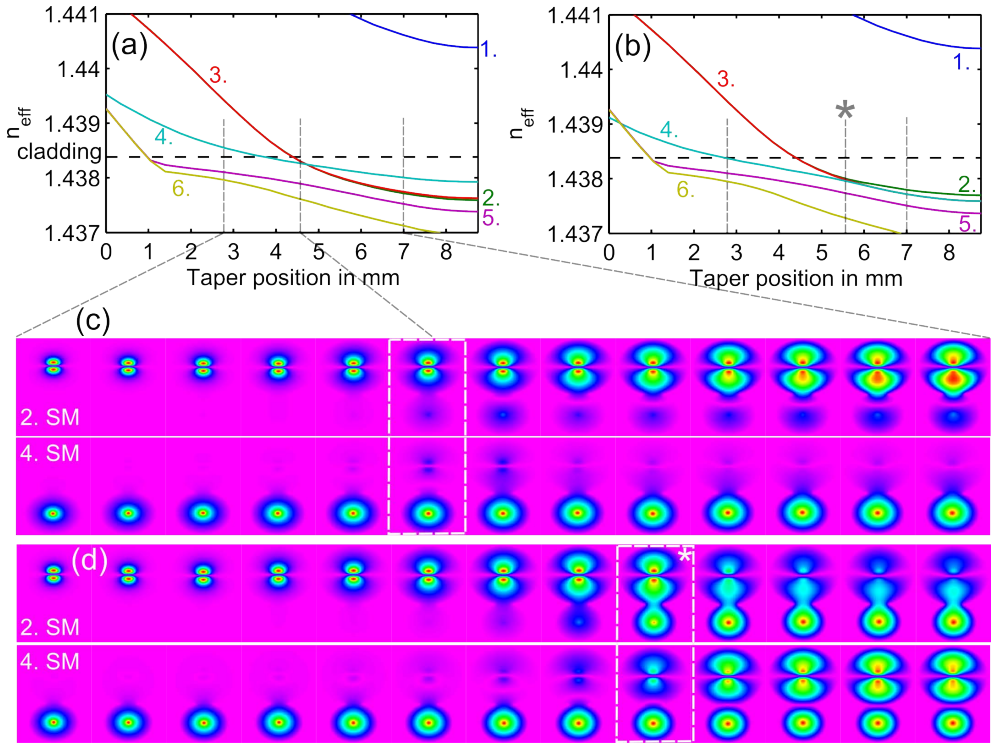

Fig. 9. Evolution of the effective refractive index n_{eff} of the n-th SM along the taper position for a coupler with a DoF of 1.95 and a pretaper length of (a) 3.5 mm and (b) 5.37 mm and otherwise with the same parameters used in Fig. 6. Second and fourth SM along the propagation in the coupler for a pretaper length of 3.5 mm (c) and 5.37 mm (d). The simulated cross section is consecutively rescaled.

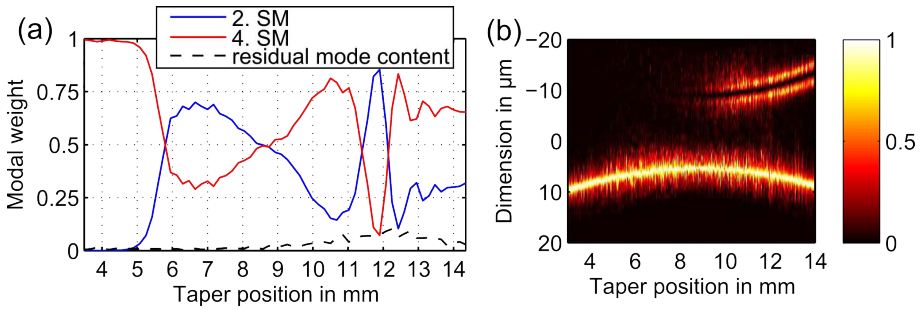

Fig. 10. Modal excitation (a) and light propagation (b) along a coupler with an extension of 10.6 mm and a pretaper length of 5.37 mm and a DoF of 1.95.

#237721 Received 8 Apr 2015; revised 28 Jul 2015; accepted 4 Aug 2015; published 24 Aug 2015

the coupler the LP_{11} mode is excited with a ratio of 30 % which is also visible in the respective light propagation (cf. Fig. 10(b)). In this case no mode beating occurs, since it is the beginning of the first coupling cycle.

The simulation results confirm the experimental observation that the coupling behavior is very sensitive to variations in the coupler geometry. The relevant parameters are the cladding diameter, pretaper length and the DoF, whereby all three parameters must be chosen adequately for the fabrication. The cladding diameter of the fibers can be measured exactly prior to the fabrication process and also the pretaper length can be applied reliably. However, the degree of fusion is difficult to control during the fabrication and cannot be simply adjusted, since it depends on the heat distribution in the crucible during the fusion process. Therefore, it is challenging to find the correct parameter set and to successfully apply it. Due to this, the presented numerical simulations can provide useful information for the fabrication of arbitrarily fused MSFCs.

4. Summary

We have analyzed the modal evolution in arbitrary fused-type mode-selective fiber couplers designed for the excitation of higher-order modes. Couplers exciting the LP_{11} mode with an efficiency of 80 % at a wavelength of 905 nm were fabricated. This was achieved by defined tuning of the coupler geometry in terms of cladding diameter, pretapering and degree of fusion. Fibers were etched to a cladding diameter of 45 µm, in order separate the effective refractive indices of the super-modes in the coupling region. An appropriate pretaper length was applied on the single-mode fiber enabling a power transfer and the excitation of the LP_{11} mode at the few-mode fiber output. In addition, it was shown that the degree of fusion has a major impact on the coupling behavior and as a consequence the applied pretaper length has to be adapted respectively.

Numerical simulations were performed to estimate fabrication parameters and to discuss the impact of variations in the coupler geometry on the super-modes and their modal weighting. Arbitrarily fused MSFC were theoretically discussed based on the super-mode coupling approach without the need to assume independent waveguides. The simulations agree qualitatively with the experimentally observed increase of maximum coupled power and the excitation of the LP_{11} mode. The evolution of the super-modes along the propagation in the taper showed that it can be achieved by adequate pretapering that the n_{eff} curves interact with each other once the super-modes become cladding modes of the tapered structure. In that case the initially excited SM and the LP_{11}-corresponding SM expand into the whole coupler structure. Therefore, the form of the super-modes is determined by the geometric structure which is defined by the cladding diameter, the pretaper length and the degree of fusion. A modal decomposition was performed and confirmed the excitation of the super-mode in the taper waist which corresponds to the LP_{11} mode.

These findings allow for a profound understanding of the coupling mechanisms in fiber couplers and enable the fabrication of novel and special fused fiber components.

Acknowledgments

This work was supported by the German Research Foundation through funding the Cluster of Excellence Centre for Quantum Engineering and Space-Time Research (QUEST). We would like to thank Andreas Grunewald for preparing the etched fibers and Henrik Tünnermann for the development of the 3D-BPM code.

#237721 Received 8 Apr 2015; revised 28 Jul 2015; accepted 4 Aug 2015; published 24 Aug 2015